Int. J. Heat Mass Transfer. Vol. 12, pp 1081–1095. Pergamon Press 1969. Printed in Great Britain

CALCULATIONS OF STEADY STATE DROPLET VAPORIZATION AT HIGH AMBIENT PRESSURES†

JOSE A. MANRIQUE and GARY L. BORMAN
Department of Mechanical Engineering, The University of Wisconsin, Madison, Wisconsin

(*Received* 3 *September* 1968 *and in revised form* 21 *February* 1969)

Abstract—A mathematical model of a spherically symmetric quiescent droplet undergoing quasi-steady vaporization in the region of its thermodynamic critical point was investigated. By steady state it is implied that all the energy arriving at the droplet surface is carried away entirely by the mass transfer. Calculated steady state temperatures and rates of vaporization of a liquid carbon dioxide droplet vaporizing in a nitrogen atmosphere are reported for ambient temperatures of 500–1600°K and pressures of 70–120 atm. The calculations include the effects of non-ideal mixtures, solubility of nitrogen in the carbon dioxide liquid, variation of the properties through the boundary layer, the effect of total pressure on vapor pressure, and the non-ideality of the enthalpy of vaporization. All of these effects were found to be important. The theory indicates that at sufficiently high pressures, steady state conditions cannot be attained. This implies that the droplet vaporizes unsteadily from its injection conditions until complete vaporization takes place. At a fixed pressure, the thermal boundary layer increases with increasing ambient temperature and at a fixed droplet temperature decreases with increasing total pressure. The steady state mass vaporization rate increases with increased pressure and/or increased ambient temperature. The droplet temperature increases slowly with ambient temperature, the rate of increase being slowest in the region near the critical pressure.

NOMENCLATURE

$A, a, B, b,$ parameters in Redlich–Kwong equation of state;
$c,$ total molar concentration [g-mole/cm^3];
$c_i,$ molar concentration of component i [g-mole/cm^3];
$c_{pi},$ molar specific heat of component i at constant pressure [cal/g-mole °K];
$\bar{c}_{pi},$ partial molal specific heat of component i [cal/g-mole °K];
$D_{AB},$ binary diffusivity for system A–B [cm^2/s];
$f_i,$ fugacity of component i [atm];
$H_i,$ enthalpy of component i [cal/g-mole];
$\bar{H}_i,$ partial molal enthalpy of component i [cal/g-mole];
$h,$ parameter in Redlich–Kwong equation of state;
$J_i,$ molar flux of species i relative to the molar; average velocity [g-mole/cm^2 s];
$k,$ thermal conductivity [cal/cm s °K];
$m,$ constant defined by equation 21 [g-mole/cm s];
$N_i,$ molar flux of species i with respect to stationary coordinates [g-mole/cm^2 s];
$P,$ total pressure, atm;
$P_{ci},$ critical presure of component i, atm;
$P_v,$ vapor pressure, atm;
$R,$ gas constant [atm cm^3/g-mole °K] or [cal/g-mole °K];
$r,$ radial distance in spherical coordinates [cm];
$r^*,$ radial distance near edge of thermal boundary layer [cm];

† This research was conducted under the sponsorship of the National Aeronautics and Space Administration, Grant No. NsG-601.

T, temperature [°K];
$\tilde{T}$, temperature for $r \geqslant r^*$ [°K];
T_{ci}, critical temperature of component i [°K];
T_{cij}, critical temperature characteristic of the i–j interaction [°K];
t, time [sec];
t_v, vaporization time [sec];
v, molar volume [cm^3/g-mole];
v_{ci}, critical volume of component i [cm^3/g-mole];
v_{cij}, critical volume characteristic of the [i–j]; interaction [cm^3/g-mole];
w, molar flow rate of the diffusing vapor [g-mole/s];
x_i, mole fraction of component i;
$\tilde{x}_i$, mole fraction of component i for $r \geqslant r^*$;
z, compressibility factor.

Greek symbols

λ, latent heat of vaporization [cal/g-mole];
Ω_a/Ω_b, dimensionless constants in the Redlich-Kwong equation of state;
ω, acentric factor.

Superscripts

l, liquid phase;
0, value in the ideal gas state;
v, vapor phase.

Subscripts

A, species A;
B, species B;
i, component i;
j, component j;
0, droplet surface;
∞, ambient conditions.

INTRODUCTION

IN HIGH pressure combustion chambers, such as those encountered in Diesel engines and liquid propellant rocket motors, the influence of the droplet vaporization process on engine performance is of primary importance. While many investigations of droplet vaporization have been carried out in the past, relatively few have dealt with high pressure environmental conditions where the droplets may approach their thermodynamic critical point. Spalding [1] analyzed the combustion of fuel droplets at supercritical pressures using a point source model and the theory of unsteady heat conduction. More recently, Rosner [2] has modified the Spalding model by taking into account the finite dimensions of the droplet. The underlying assumption in [1] and [2] is that the droplet rapidly becomes a dense vapor and subsequently burns like an initially well defined "puff of gas". Wieber [3] applied a low pressure quasi-steady vaporization model to investigate vaporization in the region of the critical point. He concluded that a fuel droplet in a rocket chamber can reach its critical temperature before the vaporization process is completed and that small pressure disturbances may lead to combustion instability in this region. However, none of these investigations have taken into account the non-ideal effects which are encountered at high pressures and the effects of pressure on the physical properties. The purpose of this investigation is thus to obtain a more basic understanding of the vaporization process in the region of the critical point and to take into account the non-ideal effects. Such a treatment although complicated by uncertainties in the determination of thermodynamic and transport properties which may exhibit anomalous behavior near the critical point nevertheless should provide a means for understanding the experimental data as it becomes available.

Although the heating-up period in the vaporization process plays an important role, only steady state conditions are considered here in order to simplify the analysis. By steady state, it is implied that all the energy arriving at the droplet surface is carried away by the mass transfer while the droplet remains at a constant temperature.

The basic relationships are first derived in a generalized form for a binary system. These relationships are then applied to a liquid carbon dioxide droplet undergoing quasi-steady vaporization in a nitrogen atmosphere. This selection of components was made because both are non-polar and of relatively simple molecular structure.

THEORETICAL MODEL

In order to simplify the analysis and concentrate on the non-ideal effects, spherical symmetry is assumed. This means that gravitational and hydrodynamic effects are neglected. The entire liquid droplet is assumed to be at a uniform constant temperature and absorption of nitrogen into the liquid phase is assumed to be confined to a thin layer at the droplet surface. Equilibrium is assumed at the liquid-vapor interface when calculating the thermodynamic properties there. Only unidirectional ordinary diffusion taken into account and the system is considered to be non-reacting. Viscous dissipation, radiant energy exchange, and the Dufour energy flux are neglected.

With these assumptions the effect of droplet surface regression is neglected. Hence, the vaporizing droplet is approximated by a porous sphere supplied with liquid from its interior.

In the analysis that follows, species A and B refer to those of the diffusing vapor and stagnant environment, respectively.

An energy balance on a spherically symmetric shell surrounding the droplet leads to the following differential equation

$$\frac{\mathrm{d}}{\mathrm{d}r}(r^2 N_A \bar{H}_A) = \frac{\mathrm{d}}{\mathrm{d}r}\left(r^2 k \frac{\mathrm{d}T}{\mathrm{d}r}\right), r > r_0 \qquad (1)$$

where $\bar{H}_A$, the partial molal enthalpy of component A, and k, the thermal conductivity of the gaseous mixture, are in general functions of temperature, pressure, and composition. This relation equates the energy transferred by the mass motion to that transferred by heat conduction.

A mass balance on a spherical shell surrounding the droplet leads to

$$\frac{\mathrm{d}}{\mathrm{d}r}(r^2 N_A) = 0, \qquad r > r_0. \qquad (2)$$

Equation (2) shows that the mass flow rate of the diffusing vapor is constant with respect to the radial distance. The molar flux of A relative to stationary coordinates, assuming that the molar flux of component B is relatively small compared to the one of A, is given by [4]

$$N_A = J_A/(1 - x_A) \qquad (3)$$

where J_A, the molar flux of A relative to the average molar velocity of the mixture is given by Fick's first law for ordinary diffusion:

$$J_A = -cD_{AB}\frac{\mathrm{d}x_A}{\mathrm{d}r}. \qquad (4)$$

This is a defining equation for the binary diffusivity D_{AB}. Although there are many alternative forms of equation 4, the form above is used in this work because it does not have limitations [5].

The error in neglecting the motion of the droplet surface may be estimated by calculating the ratio of molar fluxes at the interface. The actual molar flux of component B may be approximated by $N_B = cx_B\,\mathrm{d}r_0/\mathrm{d}t$. Furthermore, by continuity, the molar flux of the diffusing vapor is $N_A = -c_A^l\,\mathrm{d}r_0/\mathrm{d}t$. Hence, it follows that

$$|N_B/N_A| = (1 - x_A)\,c/c_A^l, r = r_0. \qquad (5)$$

For a given value of total pressure in the system, as the droplet temperature increases the density ratio, c/c_A^l, increases but the concentration of component B, $(1 - x_A)$, decreases. In the range of environmental conditions studied here, the flux ratio varies from 5 to 17 per cent.

It should be noted that an accurate description of the absorption of B into liquid A requires a knowledge of the coefficient of diffusion in the liquid phase. In the absence of such data only limiting cases are considered.

Since the total pressure is essentially constant, by the chain rule

$$\frac{d\bar{H}_A}{dr} = \frac{\partial \bar{H}_A}{\partial x_A}\frac{dx_A}{dr} + \bar{c}_{pA}\frac{dT}{dr} \tag{6}$$

and

$$\frac{dk}{dr} = \frac{\partial k}{\partial x_A}\frac{dx_A}{dr} + \frac{\partial k}{\partial T}\frac{dT}{dr} \tag{7}$$

where the stoichiometric relation $x_A + x_B = 1$ must be satisfied.

Using these expressions the equations of change become

$$\frac{d^2T}{dr^2} + \left(\frac{2}{r} + \frac{1}{k}\frac{\partial k}{\partial T}\frac{dT}{dr} + \frac{1}{k}\frac{\partial k}{\partial x_A}\frac{dx_A}{dr} - \frac{w}{4\pi r^2 k}\bar{c}_{pA}\right)\frac{dT}{dr} - \frac{w}{4\pi r^2 k}\frac{\partial \bar{H}_A}{\partial x_A}\frac{dx_A}{dr} = 0 \tag{8}$$

and

$$\frac{d}{dr}\left(-\frac{r^2 c D_{AB}}{1 - x_A}\frac{dx_A}{dr}\right) = 0 \tag{9}$$

or integrating equation (9)

$$4\pi r^2 N_A = w = \frac{-4\pi r^2 c D_{AB}}{1 - x_A}\frac{dx_A}{dr}. \tag{10}$$

To determine their boundary conditions, it is required that

$$x_A = 0 \quad \text{at} \quad r = \infty. \tag{11}$$

Furthermore, the temperature of the environment is specified as

$$T = T_\infty \quad \text{at} \quad r = \infty. \tag{12}$$

The boundary conditions at the droplet surface require special consideration. Assuming small departures from equilibrium at the interface, the concentration of species A in the gas phase, expressed as mole fraction, may be represented by the vapor-liquid equilibrium relationship:

$$x_{A0} = x_{A0}(T_0, P) \quad \text{at} \quad r = r_0 \tag{13}$$

where T_0 is the droplet temperature and P is the total pressure.

Under steady state conditions, all the energy transferred to the droplet surface by heat conduction is carried away entirely by the mass transfer. Hence it follows that:

$$4\pi r_0^2 k\frac{dT}{dr} = w(\bar{H}_A^v - \bar{H}_A^l) \text{ at } r = r_0 \tag{14}$$

Before proceeding to the evaluation of both boundary conditions (13) and (14), let us analyze some simplifying assumptions.

One commonly used approximation for equation (13) is to express the mole fraction of component A in the gas phase, at the interface, as the vapor pressure of pure component A at the equilibrium temperature T_0 divided by the total pressure, i.e.,

$$x_{A0} = P_v(T_0)/P \quad \text{at} \quad r = r_0. \tag{15}$$

This equation assumes that B is insoluble in A, that the equilibrium vapor pressure of pure component A is not affected by the presence of gas B, and that the gaseous mixture obeys the equation of state for ideal gases. It will be shown later that this relationship is far from being correct at the pressure levels encountered in the critical region.

Another approximation commonly used is to replace the term $(\bar{H}_A^v - \bar{H}_A^l)$ in equation (14) by the latent heat of vaporization of pure component A, evaluated at the equilibrium temperature T_0. This is an oversimplification at high total pressures. The term $(\bar{H}_A^v - \bar{H}_A^l)$ is the amount of heat absorbed per mole when component A evaporates from the liquid solution into the gaseous mixture, at T_0 and P, whereas λ is the heat required to evaporate a pure substance from liquid into its vapor, at T_0 and $P_v(T_0)$.

The trends predicted by the use of these simplified boundary conditions, although perfectly valid at low pressures, fail to be correct at high pressures. Now, for thermodynamic equilibrium at the interface, besides the temperature and pressure being equal in both phases, the fugacity (or chemical potential) of every com-

ponent must be the same in both phases, i.e.,

$$\begin{aligned} T &= \text{constant} \\ P &= \text{constant} \\ f_A^v &= f_A^l \\ f_B^v &= f_B^l. \end{aligned} \tag{16}$$

To solve the equations of change and their boundary conditions, a suitable equation of state has to be used. The simple Redlich-Kwong equation of state has proved to be reliable and is regarded as the best two-parameter equation now available [14]. It is of the form [6]

$$P = \frac{RT}{v - b} - \frac{a}{T^{0.5} v(v + b)} \tag{17}$$

where a and b may be taken as functions of composition and depend on the particular components involved.

Boundary conditions (13) and (14) are computed basically from equations (16) and (17). The detailed working forms of the equations are presented in the Appendix.

Finally, the integration of the equations of change requires knowledge of the thermal conductivity of the mixture, k, as well as the binary diffusivity, D_{AB}, or the product cD_{AB}. Very few experimental data are available on these transport properties for high pressure gas mixtures. The correlations used in this work are presented in the Appendix with some of their limitations.

APPLICATIONS TO A CO_2–N_2 SYSTEM

The components studied in the critical region were carbon dioxide (component A) vaporizing in a nitrogen atmosphere (component B). The critical temperature of pure CO_2 is 304·2°K and its critical pressure is 72·9 atm.

First, let us consider the boundary conditions. Figure 1 shows a calculated composition-pressure diagram for constant equilibrium temperatures of 273·78°K and 288·99°K (0·90 T_{cA} and 0·95 T_{cA}, respectively). For a given isotherm, the lower side of the solid curve shows the concentration of carbon dioxide in the gas phase which is in equilibrium with a corresponding liquid phase concentration represented

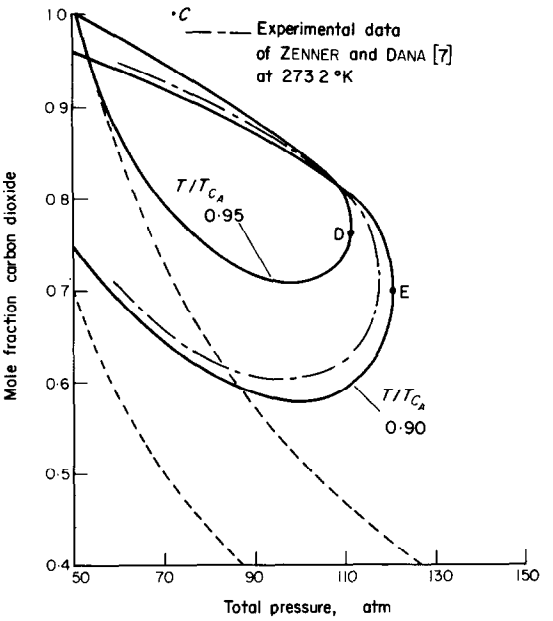

FIG. 1. Calculated vapor-liquid equilibrium isotherms for the carbon dioxide-nitrogen system. The broken lines correspond to the ideal vapor phase compositions predicted by equation (15).

by the upper side of the curve for different values of total pressure. Above a certain pressure the mole fraction of carbon dioxide in the gas phase increases rather than decreases, with the result that at still higher pressures liquid and gas phase composition become equal at the critical point. Accordingly, for a given isotherm, there exists a definite upper limit on the total pressure of the system above which steady state conditions cannot be attained. States outside the envelope enclosed by points C, D, E, . . . are intrinsically unsteady. It is observed that the range of total pressures in order to achieve steady state temperatures becomes wider as the droplet temperature (which depends also on the ambient temperature) decreases in the region of the thermodynamic critical point of carbon dioxide.

The broken lines represent the ideal vapor phase compositions predicted by equation (15). It is apparent that this relationship does not hold at high levels of total pressure.

The behavior illustrated in Fig. 1, which applies only at the interface, may be understood qualitatively for the partial molal volume of carbon dioxide reverses its sign at high pressures. Unlike the molal volume of a pure component, the partial molal volume may be either positive or negative. Since the partial molal volume of a component represents the volume change which is experienced by the entire mixture when a very small amount of that component is added at constant temperature and pressure, the gaseous mixture tends to shift its properties from a gaseous to a liquid state.

Considering the approximations involved and that only very few pure component data are required, the agreement with the experimental data of Zenner and Dana [7] is found satisfactory. Near the critical mixing point the equilibrium results are extremely sensitive to small errors in the quantities involved and as a consequence, it was found that the critical points C, D, E, . . . , are somewhat scattered.

Figure 2 shows the isothermal difference in the partial molal enthalpies of carbon dioxide

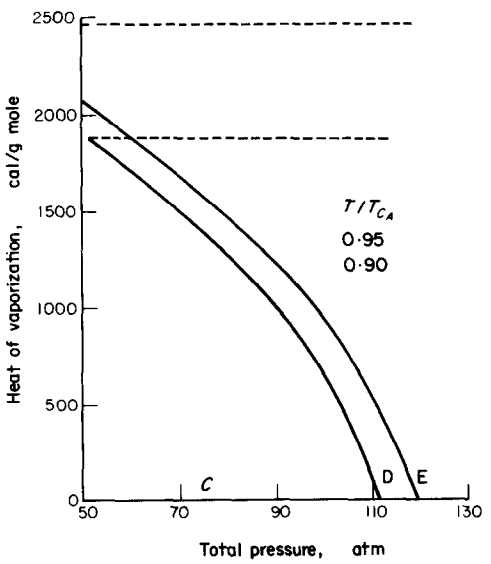

FIG. 2. Isothermal difference in the partial molal enthalpies of carbon dioxide, $(\bar{H}^v_A - \bar{H}^l_A)$, as a function of total pressure. The broken lines correspond to the latent heat of vaporization of pure CO_2, $\lambda(T)$, evaluated at the same temperatures.

across the interface, $\bar{H}^v_A - \bar{H}^l_A$, as compared to its latent heat of vaporization, λ for the same equilibrium temperatures.

At points C, D, and E of Fig. 1, the term $(\bar{H}^v_A - \bar{H}^l_A)$ becomes equal to zero since the temperature, pressure, and composition are identical in both phases. The broken lines represent the latent heat of vaporization of carbon dioxide evaluated at 273·78°K and 288·99°K by means of the generalized enthalpy deviation charts of Lydersen, *et al.* [8]. Thus, even at a subcritical temperature of carbon dioxide, the difference in enthalpies across the interface may vanish. Figure 3 shows a typical pressure-molar volume diagram for the carbon dioxide–nitrogen system.

Thus far complete thermodynamic equilibrium at the interface has been assumed. Considering that the rates of vaporization may be large enough that thermodynamic equilibrium at the interface may not be attained, let us analyze the boundary conditions and their results by assuming that nitrogen is insoluble in liquid carbon dioxide. In other words, let us postulate that very few of the nitrogen molecules in the gas phase that strike the interface have sufficient time to penetrate and become dissolved in the liquid phase.

For the case of zero nitrogen solubility, the computed values of carbon dioxide concentration in the vapor mixture are generally higher than those obtained under thermodynamic equilibrium conditions. Furthermore, the isothermal concentration of carbon dioxide starts increasing at a certain value of total pressure lower than in the corresponding thermodynamic equilibrium case (approximately 80 atm for the 273·78°K isotherm). One difficulty is encountered with this hypothesis. Since the critical points, where the temperature, pressure, and composition are the same in both phases, cannot exist as a consequence of the assumption, there is no clear transition from two to one phase states. Although the difference in enthalpies, $(\bar{H}^v_A - \bar{H}^l_A)$, across the interface does not vanish at any isotherm different from the

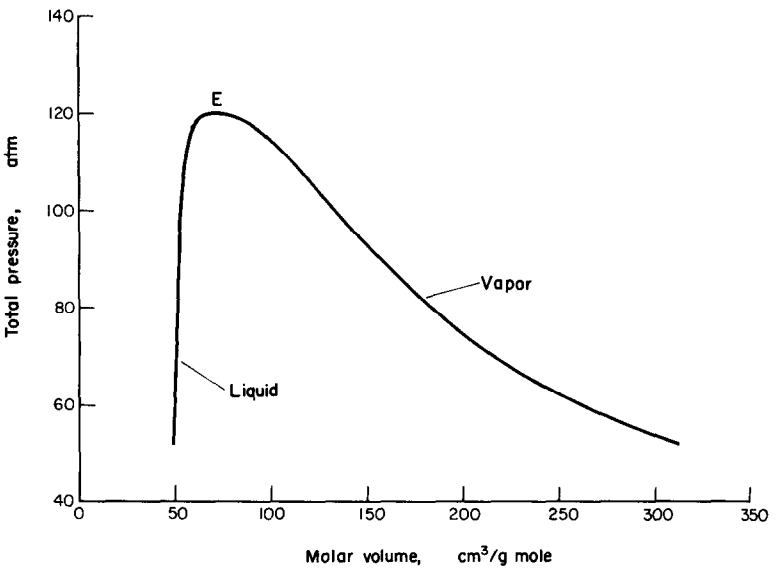

FIG. 3. Pressure-molar volume diagram for the carbon dioxide-nitrogen system at $T/T_{cA} = 0{\cdot}90$.

critical of carbon dioxide, it does follow the same trends as those predicted under thermodynamic equilibrium conditions.

Approximate calculations show that the partial molal enthalpy of CO_2 in the liquid solution is nearly the same as the one for pure liquid CO_2, at the same temperature and pressure. Thus, there is a negligibly small temperature difference between the core of the droplet and its postulated interface.

CALCULATION TECHNIQUE

The numerical integration of the equations of change throughout the nitrogen–carbon dioxide vapor film was carried out by using a recursive formula of the third category due to Heun [9]. The partial derivatives which appear in equation (8) were determined by a centered difference technique.

Setting the total pressure, the integration was initiated at the droplet surface by fixing its temperature. The rate of vaporization was iterated until the mole fraction of carbon dioxide vanished at a large distance from the droplet. The proper nitrogen temperature results. Since the ambient conditions are approached asymptotically, the numerical integration in the vapor film was carried out to a certain radial distance, r^*, where the temperature profile did not change appreciably. At this point the equations of change were modified by assuming constant k, $\bar{c}_{pA}$, and cD_{AB}, and neglecting the last term in equation (8) which is very small for $r \geqslant r^*$. These simplifications lead to the following solutions where $\tilde{x}_A$ and $\tilde{T}$ are used to indicate that they hold only for $r \geqslant r^*$,

$$\tilde{x}_A(r) = 1 - \exp.(-w/4\pi cD_{AB}r) \qquad (18)$$

and

$$T_\infty = \tilde{T}(r) + \frac{4\pi r^2 k}{w\bar{c}_{pA}} \frac{\mathrm{d}\tilde{T}}{\mathrm{d}r} \times [\exp.(w\bar{c}_{pA}/4\pi rk) - 1]|_{r=r^*}. \qquad (19)$$

When $x_A = \tilde{x}_A$ at $r = r^*$, the iterated rate of vaporization is the correct solution and the temperature of the surrounding gas can be determined accurately from equation (19).

CALCULATION RESULTS

Both temperature and concentration variations in the mixture surrounding the droplet are confined to a thin region of the order of magnitude of several droplet diameters. At a given value of total pressure the thermal boundary layer increases with ambient temperature whereas the concentration boundary layer thickness remains essentially unchanged.

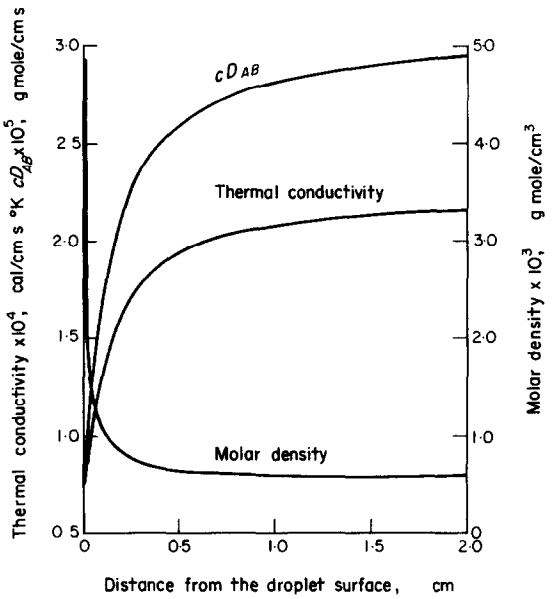

FIG. 4. Property variations in the film surrounding a 1000 μ radius carbon dioxide droplet vaporizing in nitrogen at 72·9 atm and 1595°K. Thermodynamic equilibrium at the interface is assumed.

Property variations in the film surrounding a droplet are shown in Fig. 4. For these conditions the mixture compressibility factor changes from a value of about 0·68 to unity in a small radial distance of the order of one droplet radius from the surface.

Figures 5 and 6 show that the higher the ambient temperature, the higher the rate of droplet vaporization and the higher the steady state temperature, under fixed pressure conditions. As carbon dioxide approaches its critical points, essentially no nitrogen surrounds the droplet and hence a large temperature difference between the ambient and droplet must exist so

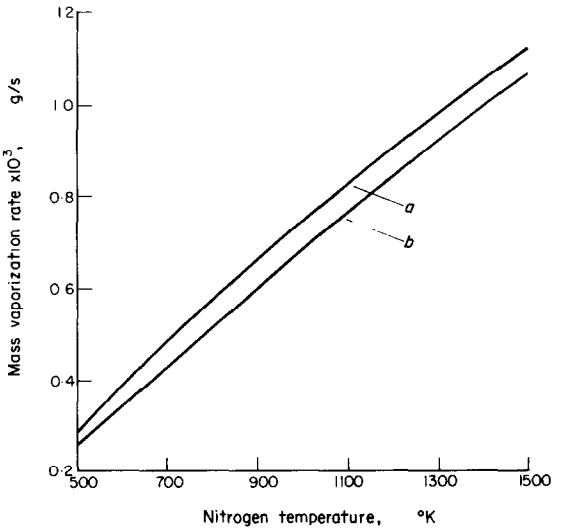

FIG. 5. Variation of mass vaporization rate with nitrogen temperature for a total pressure of 72·9 atm and a droplet radius of 1000 μ; (a) assuming thermodynamic equilibrium at the interface and (b) assuming that N_2 is insoluble in CO_2 liquid.

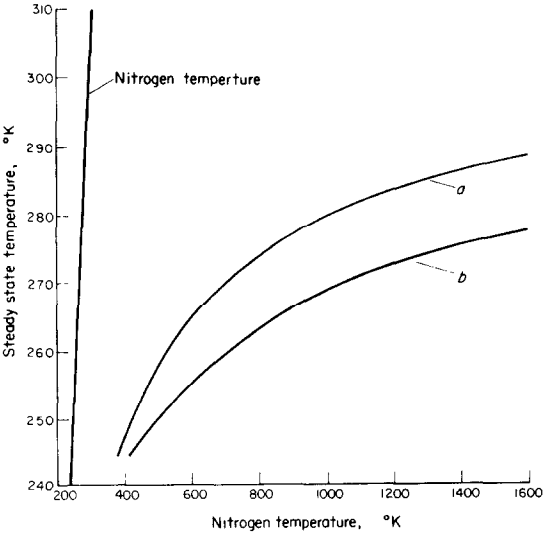

FIG. 6. Steady state temperature as a function of nitrogen temperature for a total pressure of 72·9 atm and a droplet radius of 1000 μ; (a) assuming thermodynamic equilibrium at the interface and (b) assuming that N_2 is insoluble in CO_2 liquid.

that heat may be conducted to the droplet surface. These figures also show that, for the same ambient conditions, there is a small difference between the computed steady state temperatures and mass vaporization rates by using in the model either one of the two assumptions at the interface previously discussed, i.e., thermodynamic equilibrium and no nitrogen solubility in liquid carbon dioxide. However, it should be pointed out that for values of total pressure higher than the critical pressure of CO_2, the difference between the computed steady state results is greater; e.g., at ambient conditions of approximately 84 atm and 1290°K the rates of vaporization differ by about 24 per cent and the steady state temperatures by 7 per cent. Since the equilibrium postulate is thermodynamically consistent, the results reported hereafter use this assumption.

Cross plots of steady state temperatures and vaporization rates are shown in Figs. 7 and 8. These curves are terminated on the right at the critical mixing line since points at higher pressures do not correspond to steady state solutions and can only be reached by an unsteady process. For a given liquid temperature the vaporization rate and nitrogen temperature decrease rapidly with increased pressure. The vaporization rate tends to level off and increase slightly as the critical mixing line is approached. For a given nitrogen temperature the steady state temperature and vaporization rate increase as the pressure of the system is increased. The higher the pressure, the higher the rate of increase of the steady state temperature with ambient temperature.

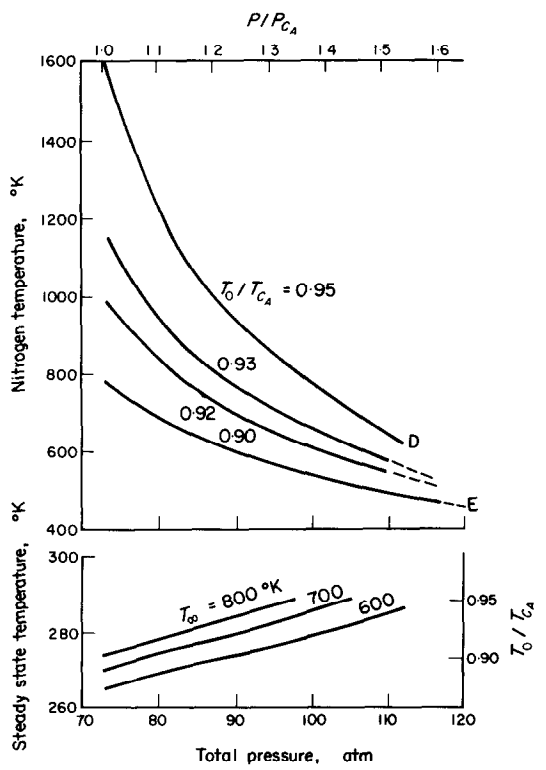

FIG. 7. Steady state temperatures under various nitrogen conditions.

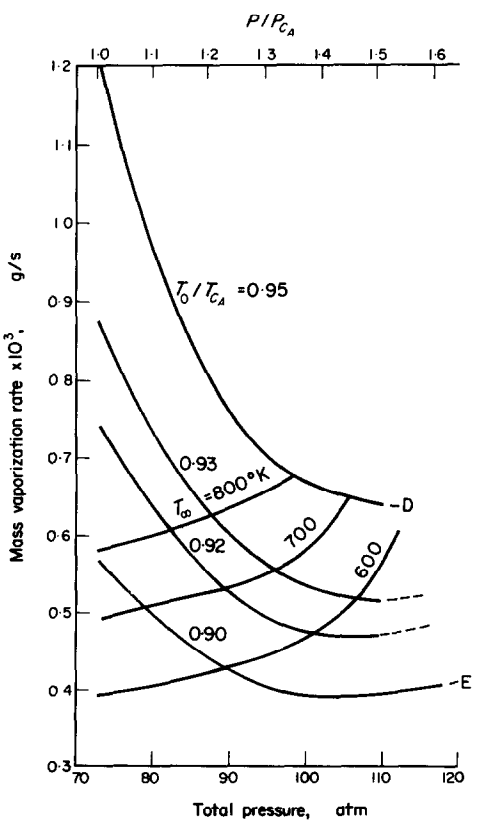

FIG. 8. Effect of pressure and temperature on mass vaporization rate. Droplet radius = 1000 μ.

Schematically, Fig. 9 indicates that for all those environmental conditions to the left of the line defined by points C, D, E, . . . , whose abscissae are determined by the critical mixing pressures (point C is fixed by the critical pressure of CO_2), the liquid droplet heats up from its injection temperature to its steady state temperature remaining at this condition until the vaporization process is completed. On the other hand, for all the ambient conditions to the right of the mentioned line, the droplet continuously heats up from its injection conditions until the vaporization process is completed.

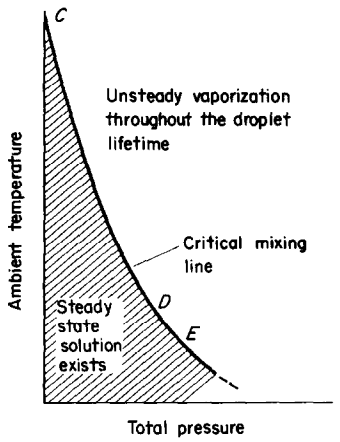

FIG. 9. Schematic diagram illustrating ambient conditions where steady state solutions exist.

Near the critical mixing line, where the change of enthalpy at the droplet interface is small, slight inaccuracies in the determination of the critical mixing pressure cause large inaccuracies in the enthalpy of vaporization and consequently, the steady state results may be affected. To analyze the overall sensitivity of the model to this inaccuracy, a change of approximately 5 per cent was made in the critical mixing pressure of the 0·96 carbon dioxide critical isotherm. This caused a difference in the enthalpy of vaporization of the order of 30 per cent at 102 atm. However, under nitrogen conditions of 850°K and 102 atm the calculated steady state results are virtually the same.

Vaporization times may be readily estimated from the foregoing results. Integrating the equation of continuity for the diffusing vapor leaving the droplet between $t = 0$ and $t = t_v$, the following expression is obtained

$$t_v = (2\pi c_A^l/m)\, r_0^2 \tag{20}$$

where the constant m is defined by

$$m = w/r_0. \tag{21}$$

Equation 20 shows that there is a linear relationship between the steady state vaporization time and the square of the droplet radius. For some given environmental conditions, the constant m may be obtained from Fig. 8 and the pure CO_2 molar density from [8].

Low pressure model

It is of interest to compare the foregoing computed results with those given by a simplified quasi-steady low pressure model which assumes constant mean physical properties and ignores all the non-idealities. Omitting the details, the solution of the simplified equations of change and their boundary conditions gives the following expressions for the steady state temperature and mass vaporization rate:

$$T_0 = T_\infty - (\lambda/c_{pA}^0)\,[\exp.\,(wc_{pA}^0/4\pi k^0 r_0) - 1] \tag{22}$$

$$w = [4\pi r_0/(T_0 c_{pA}^0 - \lambda)]\,\{(PD_{AB}^0 c_{pA}^0/R) \times \ln[P/(P - P_v)] - k^0(T_\infty - T_0)\}. \tag{23}$$

A comparison of the results predicted by equations (22) and (23) with those given in [10] showed satisfactory agreement at a total pressure of 1 atm.

Figure 10 shows the steady state temperatures and mass vaporization rates predicted by both high pressure and low pressure quasi-steady models as a function of total pressure and a nitrogen temperature of 600°K. Other steady state results under a system pressure of 72·9 atm are presented in Fig. 11.

The following conclusions may be drawn from these calculations:

(a) The low pressure model may predict more than one or no analytical solution at high pressure levels as is illustrated in Fig. 10. Although the broken line solutions may arbitrarily be considered unrealistic, the results are beclouded by the fact that the solution is not unique.

(b) At low ambient temperatures and high system pressures, the rates of vaporization predicted by the low pressure model are lower than those given by the high pressure model, e.g., at 475°K and 115 atm the low pressure model rate of vaporization is about 35 per cent lower than the high pressure model mass vaporization rate.

(c) At high ambient temperatures and a system pressure equal to the critical pressure of CO_2, the rates of vaporization predicted by the low pressure model are higher than those predicted by the high pressure model, e.g., at 1600°K and 72·9 atm the low pressure model rate of vaporization is about 22 per cent higher than the high pressure model mass vaporization rate.

The steady state temperatures predicted by the low pressure model are in general higher than those obtained with the high pressure model, under the same environmental conditions. As a consequence, the low pressure model adjusts itself to the increase in the total pressure of the system by decreasing the latent heat of vaporization and increasing the vapor pressure at the interface, along the pure CO_2 saturation curve, thus reducing in part the large property discrepancies between these models; e.g., at 600°K and 72·9 atmospheres, the increase in the steady state temperature reduces the difference in the heats of vaporization of these models from about 56 per cent to 50 per cent and the CO_2 mole fractions at the interface from approximately 32 per cent to 23 per cent.

Although the results given by both models are not completely different under the same ambient conditions, it nevertheless may be considered fortuitous that the low pressure

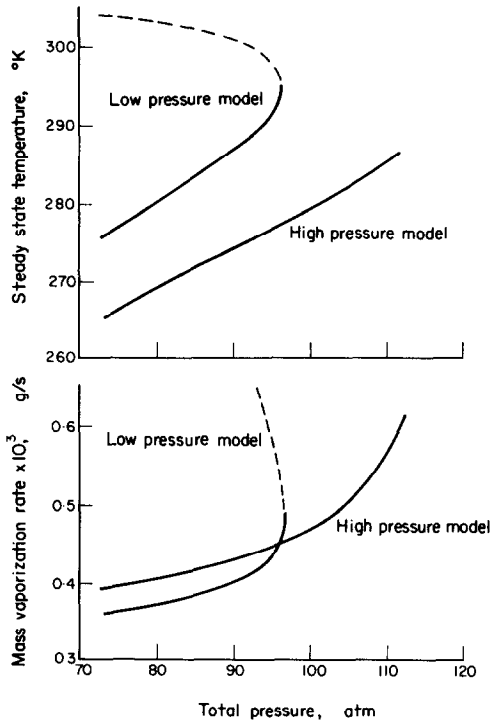

FIG. 10. Comparison of calculated steady state results by using the low pressure and high pressure models. Nitrogen temperature = 600°K, droplet radius = 1000 μ.

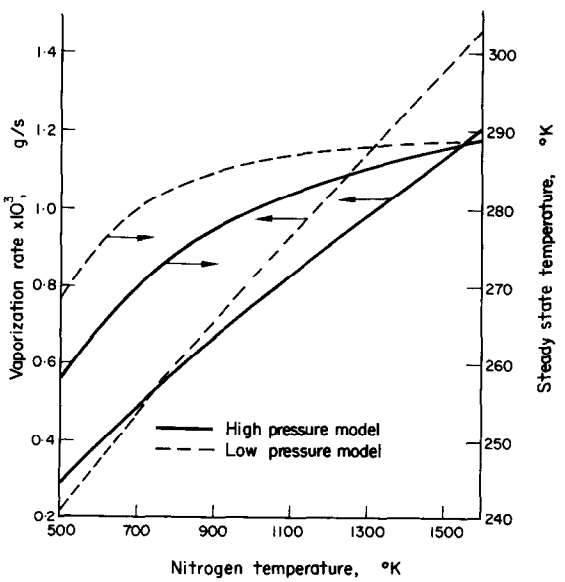

FIG. 11. Comparison of calculated steady state results by using the low pressure and high pressure models. Total pressure = 72·9 atm, droplet radius = 1000 μ.

model estimates the steady state temperatures and rates of vaporization without larger discrepancies, for the low pressure model is unrealistic in itself at high levels of total pressure.

CONCLUDING REMARKS

It is evident from the foregoing analysis that for a given value of ambient temperature there is an upper limit in the total pressure of the system above which steady state conditions cannot be attained in the vaporization process. This implies that for pressures above this limit the droplet vaporizes unsteadily from its injection conditions until complete vaporization takes place. This remark seems to be supported by recent liquid temperature measurements [11] which indicate that at high pressure levels the temperature rises continuously throughout the droplet lifetime. Therefore, supercritical temperatures may only be reached by an unsteady process.

Non-ideal effects cannot be ignored. The effect of the inert gas pressure on the vapor pressure is appreciable at high pressures and the enthalpy of vaporization is drastically modified.

By assuming constant mean physical properties, the steady state temperature is predicted without significant difference but the rate of vaporization is approximately 35 per cent higher than the corresponding variable properties case, under ambient conditions of 72·9 atm and 1600°K.

The assumption of unidirectional diffusion in the steady state regime becomes gradually less valid as the ambient temperature is decreased and the pressure in the system is increased.

In agreement with previous studies the time of vaporization spent under steady state conditions is proportional to the square of the droplet diameter.

Because experimental data is not available for comparison purposes the accuracy of the model is difficult to assess. The uncertainties in the properties of high pressure mixtures certainly may affect the absolute values reported.

Comparing the results obtained with those given by a simplified low pressure model, it is observed that the simplified model does have more than one or no analytical solutions at high pressures levels. Furthermore, under some given N_2 conditions of temperature and pressure, equations (22) and (23) predict steady state conditions which physically cannot be obtained as may be understood from Fig. 1. This clearly indicates that the low pressure model is not properly posed for high pressure environmental conditions.

ACKNOWLEDGEMENTS

The authors wish to express their deep appreciation to Professors P. S. Myers and O. A. Uyehara for their many contributions to this paper and to Mr. Paul Wieber of NASA who acted as contract monitor.

REFERENCES

1. D. B. SPALDING, Theory of particle combustion at high pressures, *ARS Jl* **29**, 825–835 (1959).
2. D. E. ROSNER, On liquid droplet combustion at high pressures, *AIAA Jl* **5**, 163–166 (1967).
3. P. R. WIEBER, Calculated temperature histories of vaporizing droplets to the critical point *AIAA Jl*, **1**, 2764–2770 (1963).
4. R. B. BIRD, W. E. STEWART and E. N. LIGHTFOOT, *Transport Phenomena*, Chap. 16. John Wiley, New York (1960).
5. E. N. LIGHTFOOT and E. L. CUSSLER, Diffusion in liquids, selected topics in transport phenomena, *Chem. Engng Progr. Symp. Ser.* **61**, 66–85 (1965).
6. O. REDLICH and J. N. S. KWONG, On the thermodynamics of solutions, *Chem. Rev.* **44**, 233–244 (1949).
7. G. H. ZENNER and L. E. DANA, Liquid-vapor equilibrium of carbon dioxide–oxygen–nitrogen mixtures thermodynamics, *Chem. Engng. Progr. Symp. Ser.* **59**, 36–41 (1963).
8. O. A. HOUGEN, K. M. WATSON and R. A. RAGATZ, *Chemical Process Principles Charts*, 3rd Edn. John Wiley, New York (1964).
9. S. H. CRANDALL, *Engineering Analysis*, Chap. III, p. 177. McGraw-Hill, New York (1956).
10. R. J. PRIEM, G. L. BORMAN, M. M. EL-WAKIL, O. A. UYEHARA and P. S. MYERS, Experimental and calculated histories of vaporizing fuel drops, NACA TN 3988, August, 1957.
11. D. P. DOMINICIS, An experimental investigation of near critical and supercritical burning of bipropellant droplets, NASA CR-72399, April, 1968.
12. R. C. REID and T. K. SHERWOOD, *The Properties of Gases and Liquids*, 2nd Edn., pp. 316, 398, 400, 463 and Appendix A. McGraw-Hill, New York (1966).

13. P. L. CHUEH and J. M. PRAUSNITZ, Calculation of high-pressure vapor–liquid equilibria, *Ind. Engng Chem.* **60**, 34–52 (1968).
14. P. L. CHUEH and J. M. PRAUSNITZ, Vapor-liquid equilibria at high pressures. Vapor-phase fugacity coefficients in non-polar and quantum-gas mixtures, *Ind. Engng Chem. Fundamentals*, **6**, 492–498 (1967).
15. W. E. STEWART, Personal communication, University of Wisconsin (1967).
16. J. V. SENGERS, Behaviour of viscosity and thermal conductivity of fluids near the critical point, critical phenomena, *Proceedings of a Conference Held in Washington, D.C.*, April, 1965, Natl. Bureau of Stds., Misc. Publ. 273, pp. 165–178 (1966).
17. L. E. STIEL and G. THODOS, The thermal conductivity of nonpolar substances in the dense gaseous and liquid regions, *A.I.Ch.E. Jl* **10**, 26–30 (1964).
18. R. S. BROKAW, Estimating thermal conductivities of nonpolar gas mixtures, *Ind. Engng Chem.* **47**, 2398–2400 (1955).
19. E. F. OBERT, *Concepts of Thermodynamics*, p. 494. McGraw-Hill, New York (1960).
20. National Bureau of Standards, Selected values of Properties of hydrocarbons, C461, p. 281 (1947).

APPENDIX

(a) *Thermodynamic Properties*

The Redlich–Kwong equation of state is

$$P = RT/(v - b) - a/T^{0.5}\, v(v + b). \quad \text{(A.1)}$$

In order to apply equation (A.1) to mixtures several mixing rules are possible.

In terms of the gaseous mixture compressibility factor, equation (A.1) was arranged in the following form [6]:

$$z = 1/(1 - h) - (A^2/B)\, h/(1 + h) \quad \text{(A.2)}$$

where

$$A = \sum_i x_i (0{\cdot}4278 T_{ci}^{2.5}/P_{ci} T^{2.5})^{\frac{1}{2}} \quad \text{(A.3)}$$

$$B = \sum_i x_i (0{\cdot}0867 T_{ci}/P_{ci} T) \quad \text{(A.4)}$$

$$h = BP/z. \quad \text{(A.5)}$$

Inspection of equations (A.1) and (A.2) shows that solving for v or z (given T, P, and x_i) involves trial-and-error calculations. Hence, for digital computer programming it is convenient to rewrite equation (A.2) as

$$z^3 - z^2 + (A^2 - B - B^2 P)\, Pz - A^2 B P^2 = 0. \quad \text{(A.6)}$$

The mixture compressibility factor was determined at each point through the boundary layer from equation (A.6) by the Newton–Raphson method. The pure component critical constants were determined from [12].

The partial molal enthalpies were determined by the following thermodynamic relation

$$(H_i^0 - \bar{H}_i)/RT^2 = \partial[\ln(f_i/x_i P)]/\partial T \quad \text{(A.7)}$$

where, in the gas phase [6]

$$\ln(f_i/x_i P) = (B_i/B)(z - 1) - \ln(z - BP) - (A^2/B)(2A_i/A - B_i/B) \ln(1 + BP/z). \quad \text{(A.8)}$$

Thus, differentiating equation (A.8) with respect to temperature, the term $(H_i^0 - \bar{H}_i)$ results.

Since equations (A.6) and (A.8) are applicable only for vapors, the mixing rules were modified to determine the vapor-liquid equilibrium at the interface and the enthalpy of vaporization. Equation (A.1) may be rearranged as

$$z^3 - z^2 + (a/T^{0.5} - BRT - b^2 P)\, Pz/(RT)^2 - abP^2/R^3 T^{3.5} = 0 \quad \text{(A.9)}$$

with the following mixing rules slightly modified from [13]:

$$a = \sum_i \sum_j x_i x_j a_{ij} \quad \text{(A.10)}$$

$$b = \sum_i x_i b_i \quad \text{(A.11)}$$

$$a_{ii} = \Omega_{ai} R^2 T_{ci}^{2.5}/P_{ci} \quad \text{(A.12)}$$

$$a_{ij} = 0{\cdot}5(\Omega_{ai} + \Omega_{aj})\, RT_{cij}^{1.5}\, v_{cij}/[0{\cdot}291 - 0{\cdot}04(\omega_i + \omega_j)] \quad \text{(A.13)}$$

$$b_i = \Omega_{bi} RT_{ci}/P_{ci} \quad \text{(A.14)}$$

$$v_{cij}^{\frac{1}{3}} = (v_{ci}^{\frac{1}{3}} + v_{cj}^{\frac{1}{3}})/2 \quad \text{(A.15)}$$

$$T_{cij} = (T_{ci} T_{cj})^{\frac{1}{2}}. \quad \text{(A.16)}$$

The pure component constants were determined from [12] and [14].

The fugacity of each component was determined by [13]

$$\ln(f_i/x_iP) = \ln[v/(v-b)] + b_i/(v-b) - (2\sum_j x_j a_{ij}) \ln[(v+b)/v]/bRT^{1.5} + [\ln[(v+b)/b] - b/(v+b)]\, ab_i/b^2RT^{1.5} - \ln(Pv/RT) \quad \text{(A.17)}$$

where the molar volume was determined via equation (A.9).

(b) *Transport Properties*

Very few experimental data are available on the binary diffusivity of high-pressure gas mixtures. In the absence of this information the product cD_{AB} was estimated from a corresponding states chart for non-polar substances based on self-diffusion measurements [15]. The method is regarded as provisional.

Contrary to the behavior in the vicinity of the critical point in the case of a pure substance, the thermal conductivity of some binary mixtures investigated [16] does not exhibit any pronounced anomaly near the critical mixing point. The absence of this anomaly seems to be established.

The thermal conductivity of the gaseous mixture was estimated by using the Stiel and Thodos pure component correlation [17] treating the mixture as a hypothetical pure component with pseudocritical properties. These pseudocritical constants were determined by using the Prausnitz and Gunn's modified rules [12]. The molar density of the mixture was computed via equation (A.6). Estimation of the mixture thermal conductivity at low pressures is required. Since it is not in general a linear mole-fraction average of the components, Brokaw's method [18] was used.

Pure component properties were obtained from [12], [19] and [20].

Résumé—Un modèle mathématique de gouttelette immobile à symétrie sphérique subissant une vaporisation quasi-permanente, a été étudié dans la région de son point critique thermodynamique. On entend par régime permanent le fait que toute l'énergie arrivant à la surface de la gouttelette est emportée entièrement par le transport de masse. Les températures calculées en régime permanent et les vitesses de vaporisation d'une gouttelette de gaz carbonique liquide se vaporisant dans une atmosphère d'azote sont données pour des températures ambiantes de 500 à 1600°K et des pressions de 70 à 120 atmosphères. Les calculs tiennent compte des effets des mélanges non-idéaux, de la solubilité de l'azote dans le gaz carbonique liquide, de la variation des propriétés à travers la couche limite, de l'effet de la pression totale sur la pression de vapeur, et de la non-idéalité de l'enthalpie de vaporisation. On a trouvé que tous ces effets sont importants. La théorie indique qu'à des pressions suffisamment élevées, les conditions du régime permanent ne peuvent être atteintes. Ceci implique que la gouttelette se vaporise d'une façon instationnaire à partir des conditions de l'injection jusqu'à ce que la vaporisation ait lieu complètement. Pour une pression fixée, la couche limite thermique augmente lorsque la température ambiante croît et, pour une température de la gouttelette fixée, diminue lorsque la pression totale augmente.

La vitesse massique d'évaporation en régime permanent augmente avec la pression et ou avec la température ambiante. La température de la gouttelette augmente lentement avec la température ambiante, la vitesse de croissance étant la plus faible dans la région au voisinage de la pression critique.

Zusammenfassung—Ein mathematisches Modell eines kugelförmigen Tropfens bei quasistationärer Verdampfung in der Nähe des thermodynamischen kritischen Punktes wurde untersucht. Durch "stationären Zustand" wird unterstellt, dass die gesamte Energie, die an die Tropfenoberfläche gelangt, durch Massentransport abgeführt wird. Es werden berechnete stationäre Temperaturen und Verdampfungsgeschwindigkeiten angegeben, für ein Kohlendioxidtröpfchen, welches in Stickstoff von 500–1600°K bei Drücken von 70–120 Atmosphären verdampft. Die Berechnung berücksichtigt den Einfluss von nicht idealen Mischungen, die Löslichkeit von Stickstoff in flüssigem Kohlendioxid, variable Stoffeigenschaften in der Grenzschicht, den Einfluss des Gesamtdruckes auf den Dampfdruck und eine nicht ideale Verdampfungsenthalpie. Alle diese Einflüsse stellten sich als wichtig heraus. Die Theorie zeigt, dass bei genügend hohen Drücken der stationäre Zustand nicht erreicht werden kann. Das bedeutet, dass das Tröpfchen

von dem Einspritzzustand bis zur völligen Verdampfung instationär verdampft. Bei festem Druck wächst die thermische Grenzschicht mit steigender Umgebungstemperatur, bei fester Tröpfchentemperatur wird sie mit steigendem Gesamtdruck dünner. Die Verdampfungsgeschwindigkeit für den stationären Zustand wächst mit steigendem Druck und/oder steigender Umgebungstemperatur. Die Tröpfchentemperatur wächst langsam mit der Umgebungstemperatur, wobei die Temperaturzunahme in der Nähe des kritischen Punktes am langsamsten ist.

Аннотация—Исследовалась математическая модель сферически симметричной неподвижной капли при квазистационарном испарении в области её термодинамической критической точки. При стационарном состоянии считается, что вся энергия на поверхности капли полностью уносится массопереносом. Приводятся расчетные температуры при стационарном состоянии и скорости испарения жидкой капли двуокиси углерода, испаряющейся в атмосфере азота при окружающей температуре 500–1600°К и давлениях от 70 до 120 атм. Расчеты учитывали влияние неидеальных смесей, растворимость азота в жидкой углекислоте, изменение свойств в пограничном слое, влияние общего давления на давление пара и неидеальность энтальпии испарения. Найдено, что все эти эффекты являются важными. Теория показывает, что при достаточно высоких давлениях нельзя достичь стационарных условий. Под этим подразумевается, что капля нестационарна от начальных условий до наступления полного испарения. При фиксированном давлении тепловой пограничный слой увеличивается с увеличением температуры окружающей среды, а при фиксированной температуре капли он уменьшается с увеличением общего давления. Скорость испарения в стационарном состоянии увеличивается с увеличением температуры или давления. Температура капли медленно увеличивается с увеличением температуры окружающей среды, причем скорость увеличения является наименьшей в области околокритического давления.